Gibbs-Thomson and diffusion-induced contributions to the growth rate of Si, InP, and GaAs nanowires

V. G. Dubrovskii,[1,2,*] N. V. Sibirev,[1] G. E. Cirlin,[1,2] I. P. Soshnikov,[1,2] W. H. Chen,[3] R. Larde,[3] E. Cadel,[3] P. Pareige,[3] T. Xu,[4] B. Grandidier,[4] J.-P. Nys,[4] D. Stievenard,[4] M. Moewe,[5] L. C. Chuang,[5] and C. Chang-Hasnain[5]

[1]*St. Petersburg Physics and Technology Centre for Research and Education, Russian Academy of Sciences, Khlopina 8/3, 194021, St. Petersburg, Russia*

[2]*Ioffe Physical Technical Institute, Russian Academy of Sciences, Politekhnicheskaya 26, 194021, St. Petersburg, Russia*

[3]*Universite et INSA de Rouen, UMR CNRS 6634, Saint Etienne du Rouvray 76801, France*

[4]*Institut d'Electronique de Microelectronique et de Nanotechnologie (IEMN), CNRS UMR 8520, Departement ISEN, 41 bd Vauban, 59046 Lille Cedex, France*

[5]*Department of Electrical Engineering and Computer Sciences, University of California, Berkeley, California 94720, USA*

(Received 30 December 2008; revised manuscript received 6 March 2009; published 19 May 2009)

We present a general model for the vapor-liquid-solid nanowire (NW) growth rates which accounts for adatom diffusion from the substrate and sidewalls into the Au catalyst drop as well as the Gibbs-Thomson effect of elevated chemical potential in the drop with a curved surface. The growth model is compared with the experimental length-diameter dependences for InP and Si NWs grown via metal organic chemical vapor deposition (MOCVD) and GaAs nanowires grown via molecular beam epitaxy (MBE). We show that MBE growth is affected mainly by adatom diffusion from the substrate, whereas MOCVD growth is affected mainly by direct Au drop impingement and sidewall diffusion. The Gibbs-Thomson effect is shown to limit growth for smaller diameter nanowires. Fits for diffusion lengths and the Gibbs-Thomson radii are determined which explain the experimental length-diameter dependence observed.

DOI: 10.1103/PhysRevB.79.205316 PACS number(s): 81.10.Aj, 68.70.+w

I. INTRODUCTION

Semiconductor nanowires (NWs) grown by the vapor-liquid-solid (VLS) mechanism are promising candidates for the use as building blocks of future nanoelectronic, nanophotonic, and nanosensing devices.[1–3] NW geometry is ideal for monolithic integration of semiconductor materials with different lattice constants due to their ability to accommodate strain in two dimensions. It is important however to understand the competing mechanisms which determine the NW growth properties,[4–15] in particular, the vertical growth rate versus radius at given set of growth conditions (Refs. 4–8 and 11–15). It has been recently shown that the length-diameter dependence of InAs NWs grown by Au-assisted metal organic chemical vapor deposition (MOCVD) is the function with one maximum, and a simplified model has been developed to explain such behavior.[11] However, the model of Ref. 11 does not regard for the fluxes directly impinging the sidewalls as well as for the sidewall diffusion, which should be prevalent during MOCVD growth. In this work we develop a general expression for the vertical growth rate of a NW which takes into account the adatom diffusion to the catalyst drop both from the sidewalls and substrate surface,[4–6] as well as the Gibbs-Thomson (GT) effect of elevation of chemical potential in the nanodrop on the NW top.[11,15] The model is used to explain experimentally observed length-diameter dependences for Si, InP, and GaAs NWs grown via MOCVD and molecular beam epitaxy (MBE) on different substrates. The fits between the model and experimental data allows us to deduce some important information concerning kinetic growth constants, in particular the diffusion lengths.

II. THEORETICAL MODEL

Our growth model is the extension of the approaches of Refs. 11 and 15, where the diffusion of surface adatoms is included but the kinetic processes on the sidewalls (adsorption, diffusion, and desorption) are completely neglected. On the other hand, the models of Refs. 5, 6, and 16, regarding for the sidewall diffusion, do not consider the substrate adatoms and, more importantly, ignore the influence of the GT effect in the drop on the resulting diffusion flux. To explain the experimental results in MBE and MOCVD of sufficiently thin NWs, the above mentioned models are generalized to consider the combined effects of (i) surface diffusion; (ii) sidewall diffusion; (iii) direct impingement onto the drop and sidewall surfaces; (iv) GT effect caused by the curvature of drop surface; and (v) continuity of chemical potential at the NW foot and at the top.

As shown schematically in Fig. 1, cylindrical NW of constant radius R is growing due to the diffusion of adatoms[4–6] and the direct impingement onto the drop surface.[7,8] The drop radius approximately equals the radius of NW. For III-V NWs, we study the case of group V reach conditions and consider the kinetics of group III (In or Ga) atoms only. Impinging flux is defined by the effective arrival rate J onto the surface and the incident angle α. The latter equals the angle of group III molecular beam to the substrate in MBE. In MOCVD, we formally put $\sin\alpha = \cos\alpha = \tan\alpha \equiv 1$ since vapors entirely surround the drop and the NW. Impinging flux in MOCVD technique is given by $J = P/\sqrt{2\pi m k_B T_v}$ with P as the partial pressure of the Si or In precursor, T_v as the vapor temperature, m as the particle mass, and k_B as the Boltzmann constant. Equivalent growth rate V is given by $V = J\Omega_s \cos\alpha$, where Ω_s is the elementary volume in the

 ©2009 The American Physical Society

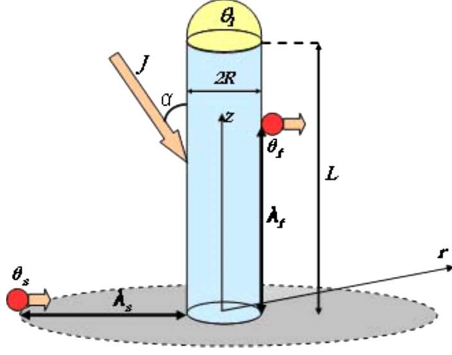

FIG. 1. (Color online) Illustration of the NW growth model with the parameters described in the text.

solid phase. The NW temperature across its length and the drop temperature are assumed as being equal to the surface temperature T. As shown in Refs. 17 for MBE and Ref. 18 for MOCVD, due to a very efficient heat exchange with the substrate, the latter acts as the thermostat and preserves a constant temperature along the NW for the lengths at least up to 10 μm. For the same reason, all adatoms are immediately thermalized at the surface temperature T upon the adsorption from the vapor phase with temperature T_v or from the molecular beam. We also neglect all thermal effects associated with the specific heats of phase transitions during the VLS growth. Drop surface in contact with the vapor is characterized by the surface energy γ. The drop can be either liquid [(VLS mechanism)[9]] or solid (vapor-solid-solid mechanism[10]); below we refer to most common VLS case. Our aim is to find general expression for the vertical growth rate of NW, dL/dt (L is the NW length and t is time), in a combined growth mode, with competition between the adatom diffusion and the GT effect in the drop.[11,15]

Stationary adatom concentrations on the substrate surface (n_s) and sidewall facets (n_f) obey diffusion equations

$$D_s \Delta n_s + J\cos\alpha - \frac{n_s}{\tau_s} = 0, \tag{1}$$

$$D_f \frac{d^2 n_f}{dz^2} + J\sin\alpha - \frac{n_f}{\tau_f} = 0. \tag{2}$$

Here, Δ is the two-dimensional Laplace operator in the substrate plane (r), z is the vertical coordinate, D_s, D_f are the diffusion coefficients, and τ_s, τ_f are the effective lifetimes on the substrate and the sidewalls, respectively. Numerical values of τ_s and τ_f are primarily determined by the rates of surface nucleation (MBE) and/or precursor decomposition rates (MOCVD). Four boundary conditions to Eqs. (1) and (2) are given by

$$\left.\frac{dn_s}{dr}\right|_{r\to\infty} = 0,$$

$$D_s \left.\frac{dn_s}{dr}\right|_{r=R} = -D_f \left.\frac{dn_f}{dz}\right|_{z=0},$$

$$\sigma_s n_s(R) = \sigma_f n_f(0),$$

$$k_B T \ln[\sigma_f n_f(L)] = \mu_l^\infty + \frac{2\gamma\Omega_l}{R}. \tag{3}$$

The first boundary condition requires that the adatom concentration is constantly far away from the NW. The second condition is simply the continuity equation at the NW foot. The third condition is imposed by the continuity of chemical potential at the NW foot, with σ_s and σ_f being the areas of elementary adsorption sites at the surface and the sidewalls, respectively. Finally, the fourth condition of continuity of chemical potential at the NW top regards for the GT effect of elevation of chemical potential in the drop with radius R, with Ω_l being the elementary volume in the (liquid) drop.[15] In Eq. (3) and hereafter the adatom ensembles are assumed as being dilute ($\sigma n \ll 1$) so that their chemical potentials amount to $k_B T \ln(\sigma n)$ for both "s" and "f" systems. The first three boundary conditions have been used previously[13] for calculation of diffusion flux to the top, while the fourth condition is modified from $n_f(L)=0$ (Ref. 13) in order to describe the GT effect in the drop.

Upon solving Eqs. (1) and (2) with boundary conditions (3), the diffusion flux to the NW top is obtained from

$$j_{\text{diff}}(L) = -D_f 2\pi R \left.\frac{dn_f}{dz}\right|_{z=L}. \tag{4}$$

Diffusion induced contribution to the growth rate, $(dL/dt)_{\text{diff}}$, is found by multiplying the diffusion flux by the factor $(\pi R^2/\Omega_s)$. After long but straightforward calculations, the exact result for $(dL/dt)_{\text{diff}}$ can be presented in the form

$$\left(\frac{dL}{dH}\right)_{\text{diff}} = \frac{2\lambda_s}{R}\left[\frac{\delta(1-\theta_l/\theta_s) + (\lambda_f/\lambda_s)\tan\alpha(1-\theta_l/\theta_f)U(L/\lambda_f)}{U'(L/\lambda_f)}\right]. \tag{5}$$

Here, $H=Vt$ is the deposition thickness, $\lambda_s=\sqrt{D_s\tau_s}$ and $\lambda_f=\sqrt{D_f\tau_f}$ are the diffusion lengths on the substrate surface and on the sidewalls, respectively (the former is usually limited by surface nucleation[11–13]), and $\delta=K_1(R/\lambda_s)/K_0(R/\lambda_s)$, where K_i is the modified Bessel function of the second kind of order i. The function $U(x)$ is given by $U(x)=\sinh(x)+\nu\delta[\cosh(x)-1]$ and $U'(x)=\cosh(x)+\nu\delta\sinh(x)$ with $\nu=(D_s\lambda_f\sigma_f/D_f\lambda_s\sigma_s)$. The quantities $\theta_s=J\tau_s\sigma_s\cos\alpha$ and $\theta_f=J\tau_f\sigma_f\sin\alpha$ denote the maximum coverage of the surface by the substrate and the sidewalls adatoms, respectively. R-dependent activity of semiconductor material in the drop is defined as $\theta_l=\exp(\mu_l^\infty/k_BT+R_{\text{GT}}/R)$, where μ_l^∞ is the chemical potential of the infinite liquid phase and $R_{\text{GT}}=(2\gamma\Omega_l)/(k_BT)$ is the characteristic Gibbs-Thomson radius.

NW growth rate is also influenced by the adsorption-desorption processes on the drop surface, directly impinged by the vapor. For a drop with contact angle close to 90°, the adsorption-desorption contribution is given by $(dL/dH)_{\text{AD}}=1-\theta_l/\theta_v$. Here, as above, θ_l is the drop activity and $\theta_v=\exp(\mu_v/k_BT)$ is the activity of the vapor phase, determined by technologically controlled growth conditions.[14,15] The resulting growth rate is the sum of diffusion and adsorption-

desorption contributions from which we must subtract the normalized growth rate of nonactivated surface V_s/V.[6] Since $1-V_s/V$ for a single NW is exactly equivalent to the probability of re-evaporation from the substrate, we have $1-V_s/V=\theta_s/\theta_v$.[15] The NW growth rate is therefore obtained in the form

$$\frac{dL}{dH} = \frac{\theta_s - \theta_l}{\theta_v} + \left(\frac{dL}{dH}\right)_{\text{diff}}, \quad (6)$$

where diffusion term is defined by Eq. (5). Among the physical parameters in Eqs. (5) and (6), the most ambiguous is the liquid activity during the growth, $\theta_l^\infty = \exp(\mu_l^\infty / k_B T)$, for which only the range of possible values is known.[15] Exact determination of μ_l^∞ requires consideration of material balance in the drop.[19]

Important particular cases of Eqs. (5) and (6) are the following. At high surface diffusivity on the sidewalls ($L/\lambda_f \to 0$), typical for MBE (Ref. 6), "formal" limit for the growth rate at $U \to 0$ and $U' \to 1$ is reduced to the result of Ref. 15:

$$\frac{dL}{dH} = \left[1 - \frac{\exp(R_{\text{GT}}/R)}{\theta_{sl}}\right]\left[\frac{1}{\theta_{vs}} + \frac{2\lambda_s}{R}\frac{K_1(R/\lambda_s)}{K_0(R/\lambda_s)}\right]. \quad (7)$$

Here, $\theta_{sl} \equiv \theta_s/\theta_l^\infty$ is the effective supersaturation of surface adatoms with respect to the liquid phase in the drop and $\theta_{vs} \equiv \theta_v/\theta_s$ is the effective vapor supersaturation with respect to the surface adatoms far away from the NW. The growth is controlled entirely by the diffusion from the substrate surface. Diffusion flux is directed to the NW top only if $\theta_{sl} > \exp(R_{\text{GT}}/R)$. The growth rate equals zero at minimum radius $R_{\min} = R_{\text{GT}}/\ln \theta_{sl}$. More accurate analysis of asymptotic behavior of Eq. (5) at $L/\lambda_f \to 0$ shows, however, that the growth rate has a more complex form given by

$$\frac{dL}{dH} = \frac{\theta_s - \theta_l}{\theta_v} + \frac{2\lambda_s}{R} \times \frac{\delta(1-\theta_l/\theta_s) + (1-\theta_l/\theta_f)[L/\lambda_s + (a\delta/2)(L/\lambda_s)^2]\tan\alpha}{1 + a\delta L/\lambda_s} \quad (8)$$

with $a = (D_s\sigma_f / D_f\sigma_s)$. Analysis of this expression will be presented elsewhere.

At low surface diffusivity ($L/\lambda_f \to \infty$), characteristic for most CVD techniques,[5,14,20] high-temperature MBE,[13] and for any growth of very long NWs ($L/\lambda_f \gg 1$), Eqs. (5) and (6) are simplified to

$$\frac{dL}{dH} = \frac{1}{\theta_{vs}}\left[1 - \frac{\exp(R_{\text{GT}}/R)}{\theta_{sl}}\right] + \left[1 - \frac{\exp(R_{\text{GT}}/R)}{\theta_{fl}}\right]\frac{2\lambda_f}{R}\tan\alpha. \quad (9)$$

Here, $\theta_{fl} \equiv \theta_f/\theta_l^\infty$ is the effective supersaturation of sidewall adatoms with respect to the drop. The first term in the right-hand side, standing for the direct impingement and the surface growth, is the same as in Eq. (7), while the diffusion induced contribution is now determined by the sidewall adatoms. Corresponding diffusion flux is positive if $\theta_{fl} > \exp(R_{\text{GT}}/R)$ and equals zero at $R_{\min} = R_{\text{GT}}/\ln \theta_{fl}$.

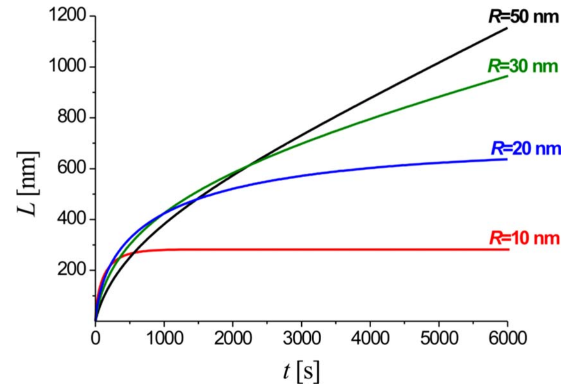

FIG. 2. (Color online) Theoretical dependences of NW length L on the growth time t obtained from Eqs. (5) and (6) at fixed $\theta_v=1$, $\theta_s=1$, $\theta_f=0.5$, $\theta_l^\infty=0.48$, $\tan\alpha=0.158$, $R_{\text{GT}}=4$ nm, $V=0.326$ nm/s, $\lambda_s=100$ nm, $\lambda_f=200$ nm, $\nu=1.57$, and different $R=10$, 20, 30, and 50 nm.

While limit cases given by Eqs. (7) and (9) provide the L-independent expressions for the growth rate and, therefore, linear dependence of NW length on the time, general Eqs. (5) and (6) demonstrate nonlinear $L(t)$ behavior. This is illustrated by the curves in Fig. 2, obtained from Eqs. (5) and (6) at fixed model parameters and different R. It is seen that an exponential growth at the initial stage is generally followed by an approximately linear growth at large t. The shape of $L(t)$ dependences is different for different R so that thicker NWs can grow slower at the initial stage and faster at the linear stage [for example, $L(t)$ curves at $R=50$ and $R=10$ nm intersect after first 600 s of growth]. The growth of very thin NWs is limited by the GT effect. In our example, $L(t)$ curve at $R=10$ nm saturates at approximately 260 nm; after that 20 nm wide NW does not elongate, thus growing at the rate of the surface.

One of the general conclusion of the model, seen directly from simplified Eqs. (7) and (9), is that the length-diameter dependence at realistic values of diffusion length (more than few tens of nanometers[11–13,20]) and the GT radius (few nanometers) is the function with one maximum. The growth of very thin NWs is mainly controlled by the GT effect,[7] whereas thick NWs exhibit a conventionally decreasing diffusion-induced behavior.[4–6] This effect was recently reported in the case of Au-assisted MOCVD of InAs NWs and described by means of a simplified model.[11] We now intend to use Eqs. (7) and (9) to explain the experimentally observed growth properties of Si, InP, and GaAs NWs, fabricated with Au catalyst by MOCVD and MBE techniques on different substrates.

III. EXPERIMENT

InP NWs are grown on the GaAs(111)B substrates using colloidal Au nanodrops as catalysts in a MOCVD reactor under the VLS growth mode. The mole fractions of the group V (tertiarybutylphosphine) and group III (trimethylindium) sources were 1.91×10^{-5} and 1.17×10^{-3}, respectively, in a 12 L/min hydrogen carrier gas flow yielding a V/III ratio of 61. This ratio was found to be within a range that yields

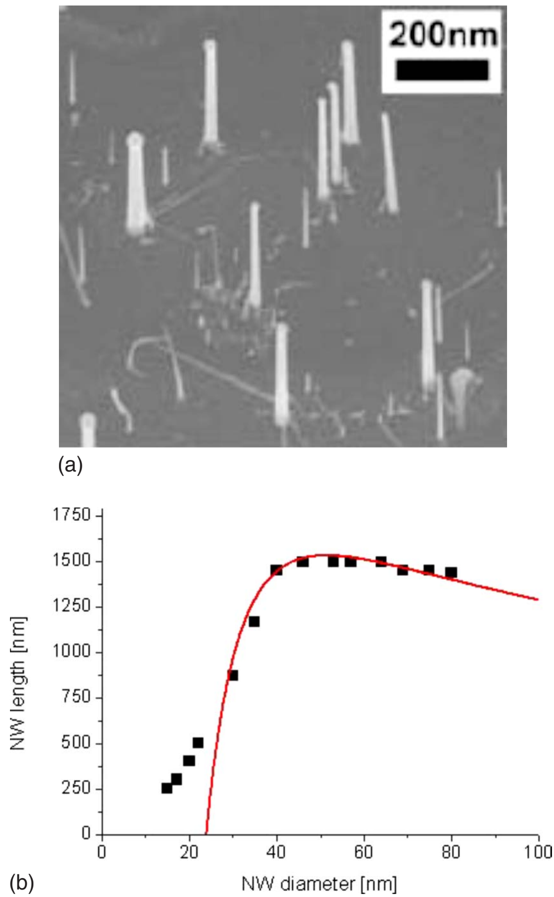

FIG. 3. (Color online) (a) SEM image of MOCVD grown InP NWs; (b) experimental length-diameter dependence (black squares) and theoretical curve (solid line) obtained from Eq. (9) at R_{GT} =4 nm, θ_{vs}=1, $\theta_{sl}=\theta_{fl}$=1.4, and λ_f=50 nm. SEM image of the sample is shown in the inset.

straight NWs with uniform diameter from base to top.[21] The growth temperature was 470 °C and the growth time was 3 min. The size of Au drops ranges from 10 to 160 nm. Analysis of high-resolution scanning electron microscopy (SEM) images [Fig. 3(a)] was used to study the length-diameter dependences, presented in Fig. 3(b).

Si NWs are grown from Si (111) substrates by MOCVD techniques with Au nanodrops as catalyst. The Au was deposited *in situ* by controlling the evaporation flow. The evaporation pressure is 7.98×10^{-10} mbar and the deposition time is 4 min. Under these conditions, two Si substrates were

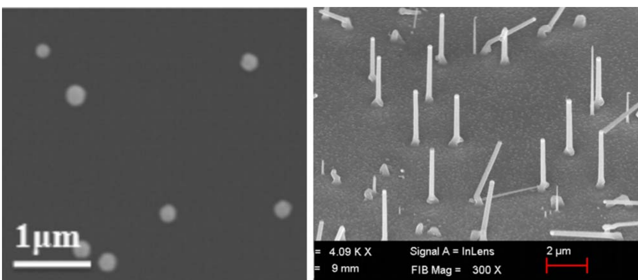

FIG. 4. (Color online) SEM images of the Si surface with low drop density (sample 1) before (left) and after (right) growth.

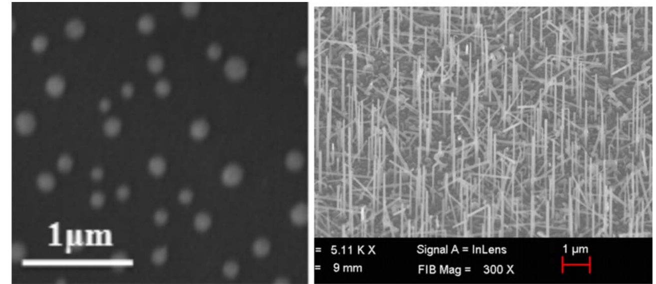

FIG. 5. (Color online) SEM images of the Si surface with high drop density (sample 2) before (left) and after (right) growth.

prepared at 460 °C and 430 °C, respectively. Corresponding SEM images of Au drops on the substrate surface before growth are shown in Figs. 4 and 5. These two substrates were used for SiNWs growth into CVD chamber. The growth temperature and time were 500 °C and 30 min, respectively. The total pressure was 1.1 mbar and SiH_4 was diluted by H_2 with the ratio of 1:150. Figures 4 and 5 show SEM images of the SiNWs in both conditions. Measurements from SEM images demonstrate that the length-diameter curve (Fig. 6) is independent on the number density of Au nanodrops at the substrate surface, which confirms the assumption of the model (single NW).

GaAs NWs were grown by MBE on the GaAs(111)B substrates by the three-step procedure.[22] First, the substrate was placed in the growth chamber of a MBE setup, where the oxide was removed from the substrates and the GaAs buffer layer was deposited. The GaAs buffer layer thickness was kept about 300 nm. Second, the samples were transferred from the MBE setup through the ambient air to the vacuum chamber equipped with an Au electron-beam evaporator. In the vacuum chamber, a thin (∼1.25 nm) Au film was deposited onto the sample surface. Third, the samples were transferred back to the MBE growth chamber and baked out at the temperature of 610 °C during 5 min in order to form the liquid alloy drops. After that, the GaAs layer with the effec-

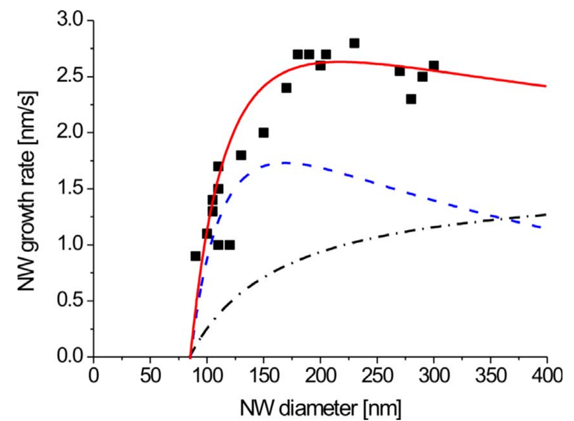

FIG. 6. (Color online) Experimental length-diameter dependence of MOCVD grown Si NWs (squares for sample 2 and circles for sample 1) and theoretical curves (lines) obtained from Eq. (9) at R_{GT}=4 nm, θ_{vs}=1, $\theta_{sl}=\theta_{fl}$=1.1, and λ_f=90 nm. Dashed-dotted line is the contribution from direct impingement, dashed line in the diffusion growth rate, and solid line is the resulting growth rate.

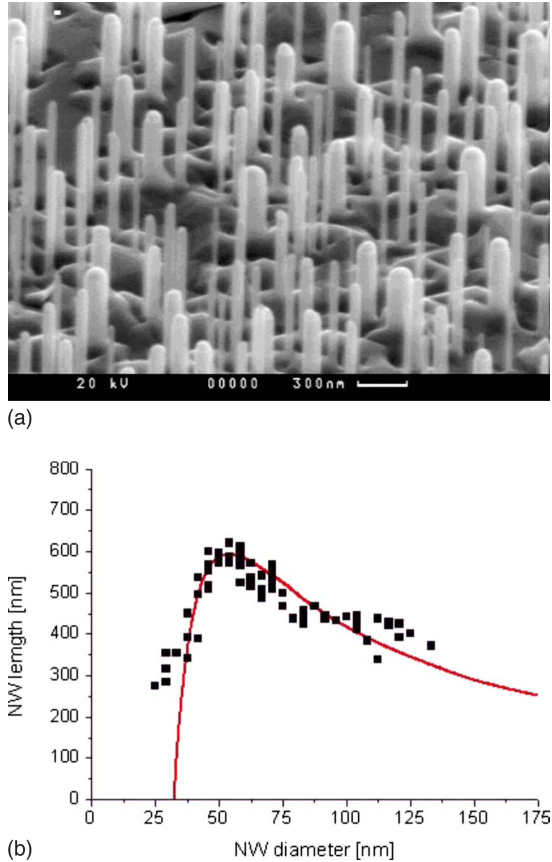

FIG. 7. (Color online) (a) SEM image of MBE grown GaAs NWs, (b) experimental length-diameter dependence (black squares) and theoretical curve (solid line) obtained from Eq. (7) at $H=420$ nm, $R_{\mathrm{GT}}=3.5$ nm, $\theta_{vs}=2.20$, $\theta_{sl}=1.24$, and $\lambda_s=95$ nm.

tive thickness of 420 nm was deposited at the deposition rate of one monolayer per second and the substrate temperature of 585 °C. The visualization of surface morphology was performed by applying SEM technique. Analysis of SEM image [Fig. 7(a)] led to the length-diameter curve shown in Fig. 7(b).

IV. RESULTS AND DISCUSSION

Since the adatom diffusion length on the sidewalls during a MOCVD growth is normally of order of 100 nm (Ref. 5) and our Si and InP NWs are normally longer than 500 nm, we use simplified Eq. (9) at $L/\lambda_f \to \infty$ for modeling of experimental length-diameter curves. Therefore, MOCVD growth of NWs is mainly promoted by the direct impingement and the sidewall diffusion, while the substrate contribution can be neglected for sufficiently tall NWs. In all our MOCVD samples, surface layer is rather thin, meaning that the precursor decomposition rate is low at the substrate surface and is chemically inhibited by the liquid Au alloy at the drop seated at the NW top. When the surface growth rate is negligible, adatoms are at the chemical potential of the vapor phase, yielding $\theta_{vs}=1$. For the same reasons, we can approximately put $\theta_{sl}=\theta_{fl}$ (or $\lambda_s \cong \lambda_f$). The value of θ_{fl} during the growth must be larger than one to ensure that the diffusion flux is directed to the NW top. The radius R_{GT} for different alloys can be estimated at given T from the known atomic volumes and surface energies of liquid Au, Si, In, and Ga (Ref. 23 and 24) (for III-V materials, we consider only group III alloys with Au because the concentration of group V elements in the drop is rather low[25]). Since the values of γ are given at temperature T_m, the surface energies at the growth temperature $\gamma(T)$ were calculated by linear approximation with corresponding coefficients $d\gamma/dT$ from Refs. 23 and 24. All these data are given in Table I. The last column presents relevant range of the GT radius with the surface energy γ and the elementary volume Ω_l between that of liquid Au (γ_{Au}) and liquid pure material (γ_{pure}). It is seen that the values of R_{GT} are between 2.2 and 4.7 nm in all the cases considered. The value of $R_{\mathrm{GT}}=4$ nm for both InP and Si NWs, used in calculations, approximately corresponds to 30% alloy of liquid In (Si) with Au.

Under the above assumptions and at known R_{GT}, Eq. (9) contains two fitting parameters, θ_{fl} and λ_f. Relative activity of sidewall adatoms θ_{fl} determines the shape of length-diameter curves for thin NWs and, in particular, the minimum diameter below which NWs would not grow. The value of diffusion length on the sidewalls λ_f mainly influences the position of the maximum and the diffusionlike decreasing part of the curve for sufficiently thick NWs. The fit for MOCVD grown InP NWs, presented by solid curve in Fig. 3 is obtained at $\theta_{fl}=1.4$ and $\lambda_f=50$ nm. The agreement between theoretical and experimental dependences is excellent for NWs longer than 500 nm. For shorter (250–500 nm in length) and thinner (~20 nm in diameter) NWs theoretical dependence is sharper than the experimental one. The predicted minimum diameter of 24 nm is therefore somewhat overestimated.[14,21] This discrepancy is mainly due to the use of a simplified Eq. (9) for all NWs, whereas the growth at the initial stage (small L) can never proceed at $L/\lambda_f \gg 1$.

Theoretical length-diameter dependence for MOCVD grown Si NWs presented by solid line in Fig. 6 is obtained at $\theta_{fl}=1.1$ and $\lambda_f=90$ nm. The adatom activity is smaller and

TABLE I. The GT radii for different alloys and material parameters.

Material	Ω_l (nm^3)	T_m (°C)	$\gamma(T_m)$ (J/m^2)	T (°C)	$d\gamma/dT$ [10^{-3} J/(m$^2\times$deg)]	$\gamma_{\mathrm{pure}}(T)$ (J/m^2)	$\gamma_{\mathrm{Au}}(T)$ (J/m^2)	R_{GT} (nm)
Au	0.0189	1065	1.145		−0.2			
In	0.0261	157	0.556	470	−0.247	0.479	1.264	2.44–4.66
Ga	0.0191	30	0.711	585	−0.07	0.674	1.246	2.24–4.1
Si	0.0181	1410	0.775	500	−0.145	0.907	1.258	3.08–4.46

the diffusion length is larger compared to the case of InP NWs. The fit is fairly good for all experimental points from 90 to 310 nm in diameter; however, nothing can be said about thinner Si NWs. Dash-dotted line in Fig. 6 is the contribution from the direct impingement and desorption from the drop. As in conventional Givargizov-Chernov model,[7] this curve is increasing with the diameter. The diffusion-induced growth rate, presented by dotted line, is the function with one maximum, determined by the competition of the adatom flux to the top and the GT effect in the drop. The curves show that the two contributions are comparable in magnitudes particularly for thicker NWs. As mentioned above, the length-radius dependences of Si NWs is independent of the NW density, which should be the case when the distance between the NWs (400 nm for the sample shown in Fig. 5) is much larger than λ_s. This again confirms the low surface diffusivity of Si adatoms on the substrate surface.

During MBE of GaAs NWs on the GaAs(111)B surface at $T=585\ ^\circ\mathrm{C}$, the adatom diffusion length on the sidewalls is very large. Different estimates provide the values of λ_f for Ga atoms on the GaAs(110) lateral surface from 3 (Ref. 25) to 10 (Ref. 26) micrometers. It is therefore reasonable to assume the effective absence of desorption from the sidewalls for NWs shorter than 700 nm (Fig. 7). Experimental length-diameter dependence was therefore fitted by simplified Eq. (7), where only the surface diffusion is taken into account. The vapor activity with respect to the surface adatoms, $\theta_{vs}=2.20$, was estimated from the data of Ref. 15. Unknown value of θ_{ls} during the growth must be larger than one, as is seen directly from Eq. (7). The value of $R_{\mathrm{GT}}=3.5$ nm, used in calculations, again corresponds to 30% alloy of liquid Ga with Au. The fit presented in Fig. 7 is obtained from Eq. (7) at $\theta_{sl}=1.24$ and $\lambda_s=95$ nm. Effective diffusion length on the GaAs(111)B surface is much smaller than the diffusion length at the vapor-solid equilibrium [$\sim$6 microns at $585\ ^\circ\mathrm{C}$ (Ref. 27)]. We can therefore conclude that λ_s is limited by the surface nucleation. This is in agreement with previous findings[4,6,13] because in MBE case a thick surface layer is formed on the nonactivated parts of the substrate. The value of 95 nm is, however, noticeably larger than our previous estimates for Ga diffusion length [$\lambda_s=25-35$ nm (Refs. 13 and 20]. This is due to accounting the GT effect in the drop and corresponding growth retardation caused by the latter.

In conclusion, we have developed theoretical model for NW growth in the combined mode, governed by a competition between the adatom diffusion and the GT effect. Exact solution for the NW growth rate has been obtained presenting the latter as function of the NW radius, the diffusion lengths, and the technologically controlled growth conditions. It has been shown that, generally, the NW length is a nonlinear function of the growth time. We have demonstrated that MOCVD growth of NWs is usually controlled by the direct impingement and the diffusion from the sidewalls, whereas the substrate contribution can be safely neglected. In opposite, in MBE technique the drop is mainly fed by the substrate adatoms, reaching the top by migrating along the sidewalls without re-evaporation. Model results is in a good agreement with the experimental length-diameter curves obtained for MOCVD grown Si, InP, and MBE grown GaAs NWs, with Au nanodrops serving as catalysts. From fitting the experimental curves, we have obtained the following values for the diffusion lengths: $\lambda_f=50$ nm (InAs NWs, MOCVD at $T=470\ ^\circ\mathrm{C}$), $\lambda_f=90$ nm (Si NWs, MOCVD at $T=500\ ^\circ\mathrm{C}$), and $\lambda_f=95$ nm (GaAs NWs, MBE at $T=585\ ^\circ\mathrm{C}$). The values of the GT radius, describing the elevation of chemical potential in the drop with a curved surface has been found to be within the range of 2.2 to 4.7 nm for the three systems considered. We now intend to investigate different growth regimes and to find unknown liquid chemical potential during the growth. We also plan to apply the growth kinetics to studying the structural zinc blende to wurtzite transformations in NWs.[14,15,25,28,29]

ACKNOWLEDGMENTS

This work was partially supported by different grants of the Russian Academy of Sciences, the Russian Federal Agency for Science and Innovation, and the Russian Foundation for Basic Research.

*dubrovskii@mail.ioffe.ru

[1] S. Gradecak, F. Qian, Y. Li, H. G. Park, and C. M. Lieber, Appl. Phys. Lett. **87**, 173111 (2005).

[2] P. J. Pauzauskie and P. Yang, Mater. Today **9**, 36 (2006).

[3] M. T. Björk, B. J. Ohlsson, T. Sass, A. I. Persson, C. Thelander, M. H. Magnusson, K. Deppert, L. R. Wallenberg, and L. Samuelson, Nano Lett. **2**, 87 (2002).

[4] L. Schubert, P. Werner, N. D. Zakharov, G. Gerth, F. M. Kolb, L. Long, U. Gösele, and T. Y. Tan, Appl. Phys. Lett. **84**, 4968 (2004).

[5] W. Seifert, M. Borgstrom, K. Deppert, K. A. Dick, J. Johansson, M. W. Larsson, T. Martensson, N. Skold, C. P. T. Svensson, B. A. Wacaser, L. R. Wallenberg, and L. Samuelson, J. Cryst. Growth **272**, 211 (2004).

[6] V. G. Dubrovskii, G. E. Cirlin, I. P. Soshnikov, A. A. Tonkikh, N. V. Sibirev, Yu. B. Samsonenko, and V. M. Ustinov, Phys. Rev. B **71**, 205325 (2005).

[7] E. I. Givargizov and A. A. Chernov, Kristallografiya **18**, 147 (1973).

[8] V. G. Dubrovskii and N. V. Sibirev, Phys. Rev. E **70**, 031604 (2004).

[9] R. S. Wagner and W. C. Ellis, Appl. Phys. Lett. **4**, 89 (1964).

[10] K. A. Dick, K. Deppert, T. Martensson, S. Mandl, L. Samuelson, and W. Seifert, Nano Lett. **5**, 761 (2005).

[11] L. E. Fröberg, W. Seifert, and J. Johansson, Phys. Rev. B **76**, 153401 (2007).

[12] V. G. Dubrovskii and N. V. Sibirev, J. Cryst. Growth **304**, 504 (2007).

[13] V. G. Dubrovskii, N. V. Sibirev, R. A. Suris, G. E. Cirlin, V. M. Ustinov, M. Tchernysheva, and J. C. Harmand, Semiconductors

40, 1075 (2006).
[14] M. Moewe, L. C. Chuang, V. G. Dubrovskii, and C. Chang-Hasnain, J. Appl. Phys. **104**, 044313 (2008).
[15] V. G. Dubrovskii, N. V. Sibirev, J. C. Harmand, and F. Glas, Phys. Rev. B **78**, 235301 (2008).
[16] J. Johansson, C. P. T. Svensson, T. Martensson, L. Samuelson, and W. Seifert, J. Phys. Chem. B **109**, 13567 (2005).
[17] F. Glas and J. C. Harmand, Phys. Rev. B **73**, 155320 (2006).
[18] A. T. Galisultanov, I. A. Fedorov, N. V. Sibirev, I. P. Soshnikov, and V. G. Dubrovskii, Tech. Phys. Lett. **34**, 512 (2008).
[19] V. G. Dubrovskii, N. V. Sibirev, G. E. Cirlin, J. C. Harmand, and V. M. Ustinov, Phys. Rev. E **73**, 021603 (2006).
[20] V. G. Dubrovskii, N. V. Sibirev, R. A. Suris, G. E. Cirlin, J. C. Harmand, and V. M. Ustinov, Surf. Sci. **601**, 4395 (2007).
[21] C. Chuang, M. Moewe, S. Crankshaw, and C. Chang-Hasnain, Appl. Phys. Lett. **92**, 013121 (2008).
[22] V. G. Dubrovskii, I. P. Soshnikov, G. E. Cirlin, A. A. Tonkikh, Yu. B. Samsonenko, N. V. Sibirev, and V. M. Ustinov, Phys. Status Solidi B **241**, R30 (2004).
[23] J. J. Jasper, J. Phys. Chem. Ref. Data **1**, 841 (1972).
[24] G. J. Janz, *Natl. Bur. Standards*, (NSRDS-NBS 28, Washington, 1969).
[25] J. C. Harmand, G. Patriarche, N. Péré-Laperne, M.-N. Mérat-Combes, L. Travers, and F. Glas, Appl. Phys. Lett. **87**, 203101 (2005).
[26] T. Takebe, M. Fujii, T. Yamamoto, K. Fujita, and T. Watanabe, J. Appl. Phys. **81**, 7273 (1997).
[27] S. Koshiba, Y. Nakamura, M. Tsuchiya, H. Noge, H. Kano, Y. Nagamune, T. Noda, and H. Sakaki, J. Appl. Phys. **76**, 4138 (1994).
[28] J. Johansson, L. S. Karlsson, C. P. T. Svensson, T. Mårtensson, B. A. Wacaser, K. Deppert, L. Samuelson, and W. Seifert, Nature Mater. **5**, 574 (2006).
[29] F. Glas, J. C. Harmand, and G. Patriarche, Phys. Rev. Lett. **99**, 146101 (2007).